Structural changes and pressure-induced chemical decomposition of boric acid

A. Yu. Kuznetsov[1], <u>A. S. Pereira</u>[2], J. Haines[3], L. Dubrovinsky[1], V. Dmitriev[4], P. Pattison[4,5]

[1]Bayerisches Geoinstitut, Universität Bayreuth, D-95440 Bayreuth, Germany

<Alexei.Kuznetsov@uni-bayreuth.de>

[2]Instituto de Física e Escola de Engenharia, Universidade Federal do Rio Grande do Sul,

91501-970, Porto Alegre, RS, Brazil <altair@if.ufrgs.br>

[3]Laboratoire de Physico-Chimie de la Matière Condensée, Université Montpellier II,

Montpellier Cedex 5, France <jhaines@lpmc.univ-montp2.fr>

[4]Swiss-Norwegian Beam Lines at ESRF, Rue Jules Horowitz 6, BP 220, F-38043 Grenoble

Cedex, France

[5]Laboratory of Crystallography, Swiss Federal Institute of Technology, BSP,CH-1015

Lausanne, Switzerland

Abstract

X-ray powder diffraction studies along with complementary Raman and infrared spectroscopy measurements disclosed the pressure-induced chemical decomposition of boric acid, H_3BO_3. The layered triclinic structure of H_3BO_3 suffers a highly anisotropic compression associated to a strong reduction of the interlayer spacing. The starting structure becomes unstable at about 2 GPa and decomposes on a cubic polymorph of the metaboric acid, HBO_2, and ice. Two structural modifications of ice, ice VI and ice VII, are formed in the course of the chemical decomposition of boric acid. X-ray diffraction data suggest a new polymorph of H_3BO_3 as a precursor structure of the decomposition process. The triclinic lattice of the new phase has a translation period corresponding to 3 layers of hydrogen-bonded $B(OH)_3$ molecules in place of the 2 layers period observed in the initial phase. The large volume variation and the important structural changes associated to the decomposition suggest a high free energy of activation. This yields a slow kinetics at room temperature, and a phase composition very dependent of the specific pressure-time path followed by the sample. Based on the obtained results a mechanism for the chemical decomposition of H_3BO_3 is proposed and the possible role of hydrogen bonds in the observed transformations is discussed.

Introduction

Boric acid (H_3BO_3) was one of the first compounds with a hydrogen bonded crystal structure to be characterized by X-ray diffraction methods. Its triclinic crystal structure, space group $P\bar{1}$, consists of a layered packing of slightly buckled sheets (Zachariasen, 1954). Each sheet is formed by H_3BO_3 molecular units with nearly perfect C_{3h} symmetry, linked together by hydrogen bonds O-H⋯O. Ab initio calculations (Zapol, 2000) show that the binding energy of sheets is about one third of the intralayer interaction energy. The relatively low energy needed to promote the mutual sliding between layers of such a structure explains the lubricant properties of boric acid. These properties are often associated to the formation of a boric acid film on the surface of boron-containing materials due to interaction of B_2O_3 with the moisture in the air (Erdemir, 1996). However, some care should be taken to describe

the behavior of a low friction coating material assuming its expected structural properties at room conditions. Lubricant materials can be subjected in applications to compression and heating, and possible changes in the properties of boric acid under such pressure-temperature conditions require an investigation.

Under heating, H_3BO_3 undergoes a dehydration process which can produce different phases according to the temperature and heating time (Kracek, 1938). The dehydration starts at 130ºC leading to the formation of HBO_2 (metaboric acid), and, at higher temperatures, B_2O_3 is produced. Metaboric acid can crystallize in three different forms: α-HBO_2 (orthorhombic), β-HBO_2 (monoclinic), and γ-HBO_2 (cubic). The cubic phase is the most stable and the densest among the crystalline forms of metaboric acid (McCalla, 2002).

In contrast to temperature-induced changes of H_3BO_3, the influence of pressure on structure and stability of H_3BO_3 have not been yet comprehensively studied. The available laboratory energy-dispersive X-ray diffraction and Raman spectroscopy studies showed that the layered structure of H_3BO_3 is highly unstable under pressure even at room temperature (Pereira, 2003). This work evidenced a transition of H_3BO_3 to a highly disordered, probably amorphous state at pressures about 2 GPa and an appearance at higher pressures of a new phase, whose diffraction pattern could be indexed with the cubic polymorph of the metaboric acid (γ-HBO_2). The observed transitions were interpreted as a novel pressure induced decomposition of H_3BO_3. However, some questions remained about a conclusive identification of the decomposition products, their structures and the possible formation of new phases of boric acid (Shuvalov, 2003) induced by pressure.

Very recent laboratory angle-dispersive X-ray diffraction and infrared spectroscopy studies undertaken by the present investigators (Pereira, to be published), conclusively demonstrated the pressure-induced decomposition of H_3BO_3 on HBO_2 and H_2O. However, the quality of the obtained X-ray diffraction data precluded the structural characterization of the compounds involved in the decomposition process. The complementary infrared data pointed to the presence of "non-interacting" H2O molecules along with the ice VI polymorph of water at the early stages of the pressure-induced decomposition.

In order to have high-quality X-ray diffraction data to elucidate the structural aspects of the pressure induced decomposition of H_3BO_3, we have performed in situ measurements using a focused beam from a 3rd generation synchrotron source. In this paper we report such results along with a complementary study by Raman and IR spectroscopy.

Experimental Procedure

The high-pressure studies of the boric acid were carried out on a reagent grade H_3BO_3 powder samples with purity 99.9% loaded in a diamond-anvil cell (DAC). Structural data were obtained at ID30 beam line at the European Synchrotron Radiation Facility (ESRF, Grenoble, France). In-situ high-pressure measurements employed angle-dispersive X-ray powder diffraction technique with monochromatic (λ=0.3738 Å) X-radiation. Diffraction patterns were collected with an image plate detector (MAR345). One-dimensional 2θ dependences of the X-ray diffracted intensities were obtained by integration of two-dimensional diffraction images using the ESRF Fit2D software (Hammersley, 1996).

The Raman scattering measurements were carried out at Bayreuth Geo-Institute using Dilor XY system with the 5145 Å Ar-ion laser as the excitation line. The incident laser power varied in the range 150-180 mW. The spectrometer was calibrated using the Γ_{25} phonon of diamond-structured Si (Fd-3m). Raman spectra were collected in the 100-4000 cm^{-1} range. The high-pressure IR measurements followed the Raman data collection at each pressure step. The IR spectra were obtained in a reflection mode on a previously described BrukerIFS 120 HR high-resolution FTIR spectrometer with a Bruker IR microscope (Bromiley, 2004). A thin platinum foil was placed in the gasket hole of DAC assemblage and was covered by the sample, providing thus a reflection surface for the incident IR radiation. The

sum of 500 scans defined each high-pressure IR spectrum in the 600-4000 cm-1 spectral region.

Results

X-ray diffraction

The known triclinic structure of boric acid (Zachariasen, 1954) described perfectly powder diffraction patterns collected from the starting H_3BO_3 sample at ambient conditions. However, the relative intensities of the diffraction peaks suffered a significant alteration at ambient pressure just after a compaction of the sample. We attribute this alteration to a preferred orientation of crystallites which develops at slight squeezing of the sample. Subsequent compression to about 2 GPa results in a continuous variation of the diffraction spectra (Figure 1). Preferred orientation effects precluded a full structural refinement; nevertheless a Le Bail fit provided an excellent description of the observed diffraction patterns in terms of the known triclinic phase of H_3BO_3. At the same time, some discrepancies between theoretical and experimental diffraction patterns could be observed at pressures above 1 GPa. A new peak, which appeared at 2θ near 4.2 degrees (indicated by an arrow in Figure 1) and a visible misfit in calculated and experimental intensities at low 2θ values indicate some structural changes and a possible new phase of H_3BO_3.
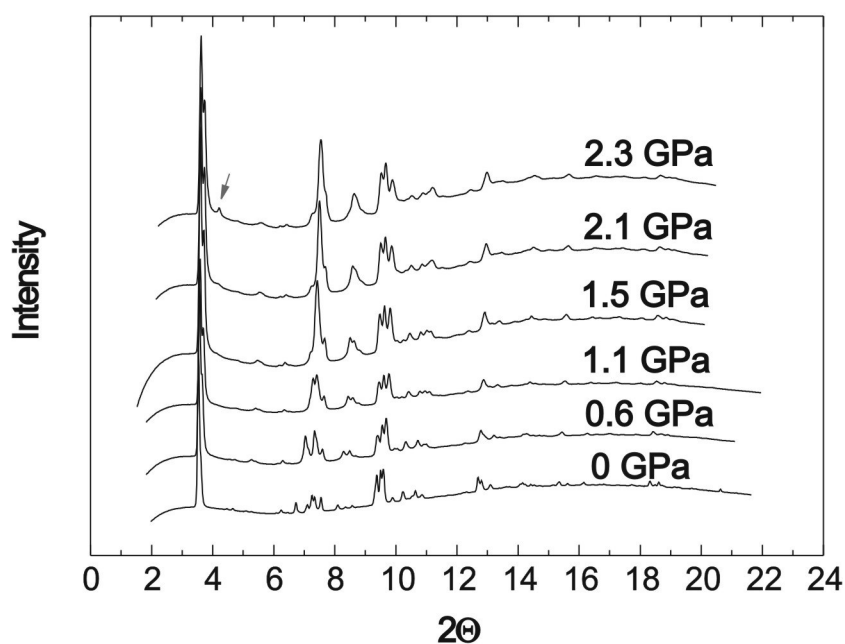

Figure 1: Evolution of the X-ray diffraction patterns for H_3BO_3 with increasing pressure. The arrow indicates the peak which can not be accounted by a triclinic lattice of the boric acid (see details in the text).

Since the overall description of the diffraction patterns in terms of the initial triclinic lattice was good, we looked for a possible candidate for the new phase of H_3BO_3 closely related to the old one. One of the possibilities can be a change in the stacking sequence of sheets of hydrogen bonded $B(OH)_3$ molecules. Figures 2a and 2b compare the theoretical and experimental diffraction patterns of the boric acid with 2 and 3 sheets per translational period c respectively. The three-layered structure accounts for the new peak and gives better reliability indices of the profile fit ($R_{wp} = 0.0072$, goodness of fit equal to 0.2702) than the two-layered structure ($R_{wp} = 0.0144$, goodness of fit equal to 1.097). This result provides evidence that in compressed H_3BO_3 the stacking sequence of sheets may not be longer the

same as at ambient conditions. It is useful to note that a three-layered periodicity has been already reported for a new trigonal polytype of the boric acid (Shuvalov, 2003).
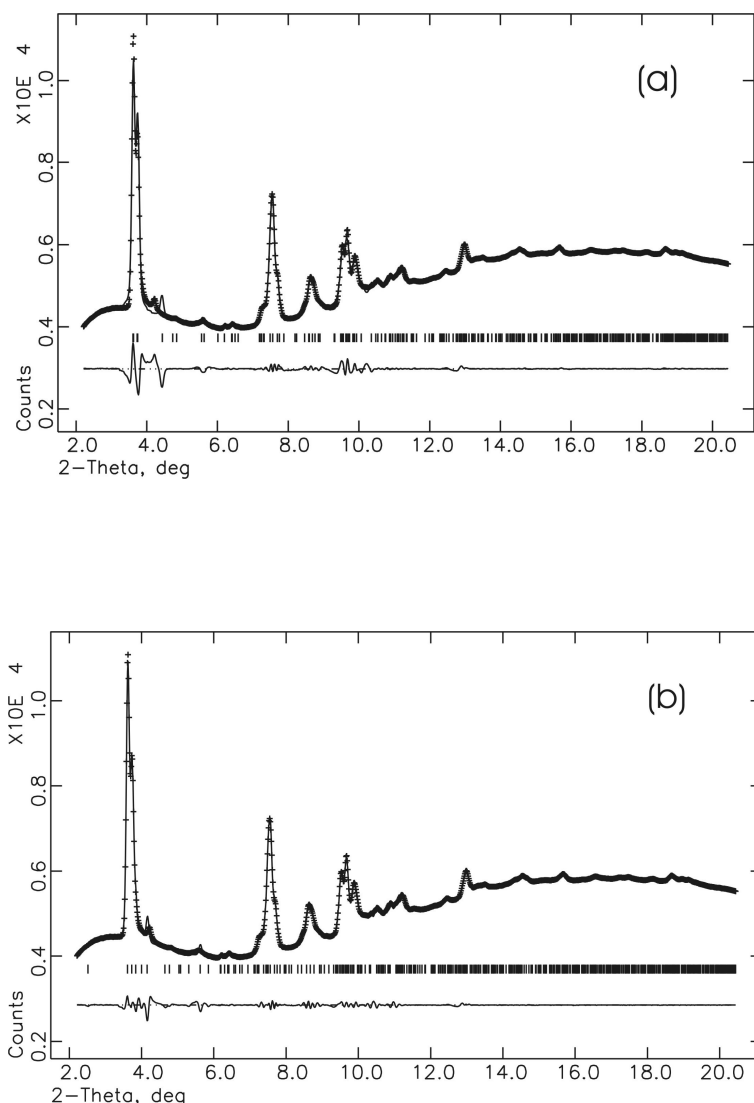

Figure 2: Experimental (crosses) and calculated (solid lines, GSAS, Le Bail fit) diffraction patterns for H_3BO_3 compound at 2.3 GPa and ambient temperature. (a) Structural model with a triclinic lattice which assumes 2 layers of hydrogen bonded $B(OH)_3$ molecules per translational period along c axis; (b) 3-layered structural model of the boric acid.

The increase of pressure to about 2 GPa results in a fast decrease of the parameter c of the triclinic lattice of H_3BO_3 compared with the respective changes of a and b lattice parameters (Figure 3). Such behavior of the lattice parameters fits well to theoretical predictions (Zapol, 2000) from which one can expect the higher compressibility of H_3BO_3 structure along crystallographic axis c than along axis a or b. The Birch-Murnaghan isothermal equation of state (Birch, 1978) was fitted to the experimental data. The numerical results of the fitting procedure [V_0=274.394(0.07) Å^3, B_0=5.3(0.6) GPa, B_0'=19(3)] reveal the overall high compressibility of the boric acid.
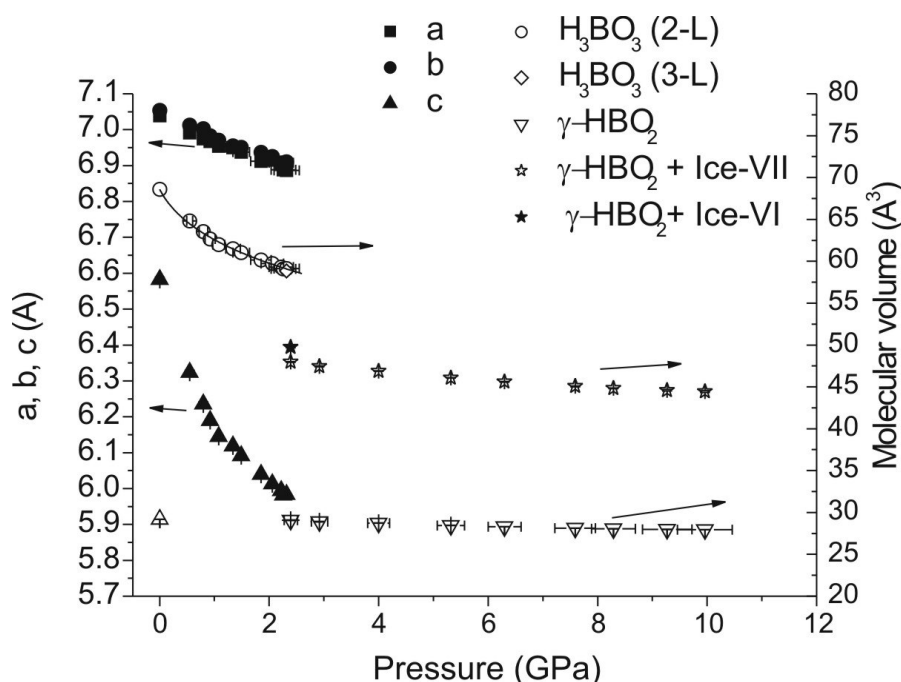
Figure 3: Pressure-induced variation of the lattice parameters of the boric acid (H_3BO_3), and of the molecular volume of H_3BO_3 and its chemical decomposition products, metaboric acid (HBO_2) and ice. Solid squares, circles and triangles are a, b, c lattice parameters of the triclinic H_3BO_3. Open circles and up-side down triangles are the molecular volumes of the triclinic H_3BO_3, and cubic HBO_2 phases. Open stars and solid star refer to the sum of the molecular volumes of HBO_2 and ice-VII phases, and to the sum of the HBO_2 and ice-VI molecular volumes respectively. Open triangle at ambient pressure represents the molecular volume of the cubic HBO_2 phase (Zachariasen, 1963). Open diamond at 2.3 GPa shows the molecular volume of a 3-layered structure of H_3BO_3.

The appearance of new reflections was clearly seen at pressures above 2 GPa. Three new phases were identified: cubic metaboric acid [γ-HBO_2, a=8.8693(3) Å), tetragonal ice-VI (a= 6.0871(8) Å, b= 5.579(2) Å) and cubic ice-VII (a=3.3552(7) Å] disclosing thus the pressure induced decomposition of H_3BO_3 on HBO_2 and H_2O at ambient temperature. Figure 4 shows the selected angle-resolved X-ray diffraction patterns of the sample, covering the decomposition process. The formation of decomposition products was accompanied by a drop of the pressure in the gasket hole. We compensated this pressure drop by a slight increase of the pressure after each data collection. The pressure was kept within 2.1-2.7 GPa range during the chemical decomposition, which took about 2 hours. The decomposition products, γ-HBO_2, ice-VI and ice-VII, perfectly accounted for all features in the final diffraction pattern at about 2.4 GPa (Figure 5). Subsequent pressure increase to about 3 GPa resulted in a HBO_2-I and ice-VII two phase mixture, which was observed up to 10 GPa, the highest pressure of the diffraction experiments. Figure 3 summarizes the variation of volumes of all observed phases. One can see that the chemical decomposition of H_3BO_3 on HBO_2 and H_2O results in a big overall volume reduction, suggesting that this pressure induced reaction is driven by density effect.
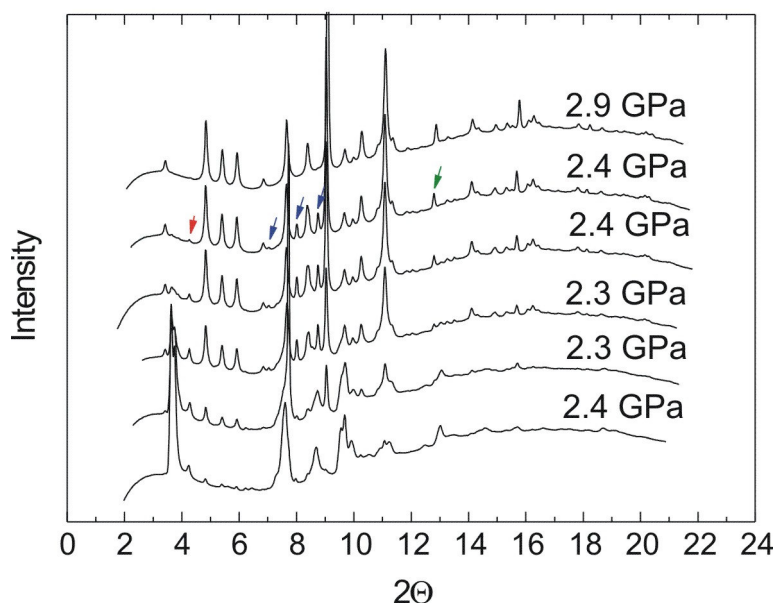
Figure 4. Evolution of the X-ray diffraction patterns for the sample of H_3BO_3 during the chemical decomposition process at average pressure about 2.3 GPa. One can observe the formation of peaks originated by ice-VI (blue arrows) and ice-VII (green arrow) phases non-overlapping with the peaks from cubic HBO_2. Red arrow indicates the new peak from H_3BO_3 phase shown in the figure 1. Peaks from ice-VI phase disappear on further compression to 2.9 GPa.
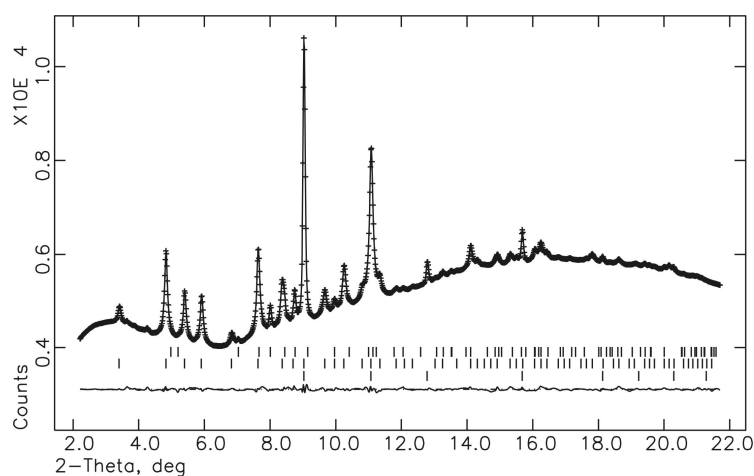

Figure 5. Experimental diffraction pattern after complete chemical decomposition of the boric acid H_3BO_3 at 2.4 GPa (crosses) and Rietveld fit (GSAS, solid line) of γ-HBO_2, ice-VI and ice-VII structures. Upper tic marks, tic marks in the middle and lower tic marks indicate the positions of the Bragg reflections for the ice-VI, γ-HBO_2 and ice-VII phases respectively.

Raman and IR spectroscopy

Raman and IR spectra (Fig. 6 and Fig. 7) obtained at ambient conditions demonstrated a good agreement with the Raman and IR spectra of the boric acid analyzed in earlier studies (Bethell, 1954; Zaki, 1995). The Raman and IR bands of this study were assigned according to the interpretations of the respective spectra given in the latter works. Based on the ideal *C3h* symmetry of the boric acid molecules and the layer unit cell which

contains two such molecules (Bethell, 1954) one can assign the strong bands in the ambient pressure spectrum of Figure 6a at 500, 880, 1167 cm^{-1} to the $\nu_{23}(E_{2g})$ in-plane O-B-O angle deformation, the $\nu_3(A_g)$ symmetric B-O bond stretching and the $\nu_{22}(E_{2g})$ in-plane O-B-H angle deformation mode respectively. The Raman bands observed at 3168 and 3245 cm^{-1} (Figure 6b, ambient pressure spectrum) correspond to the two Raman active $\nu_1(A_g)$ symmetric and $\nu_{20}(E_{2g})$ antisymmetric O-H bond stretching vibration respectively. The bands observed at ambient conditions below 400 cm^{-1} can be assigned to the lattice modes, at the same time the peak at 212 cm^{-1} can also be one of the allowed $\nu_{14}(E_{1g})$ fundamentals which was not reported earlier.
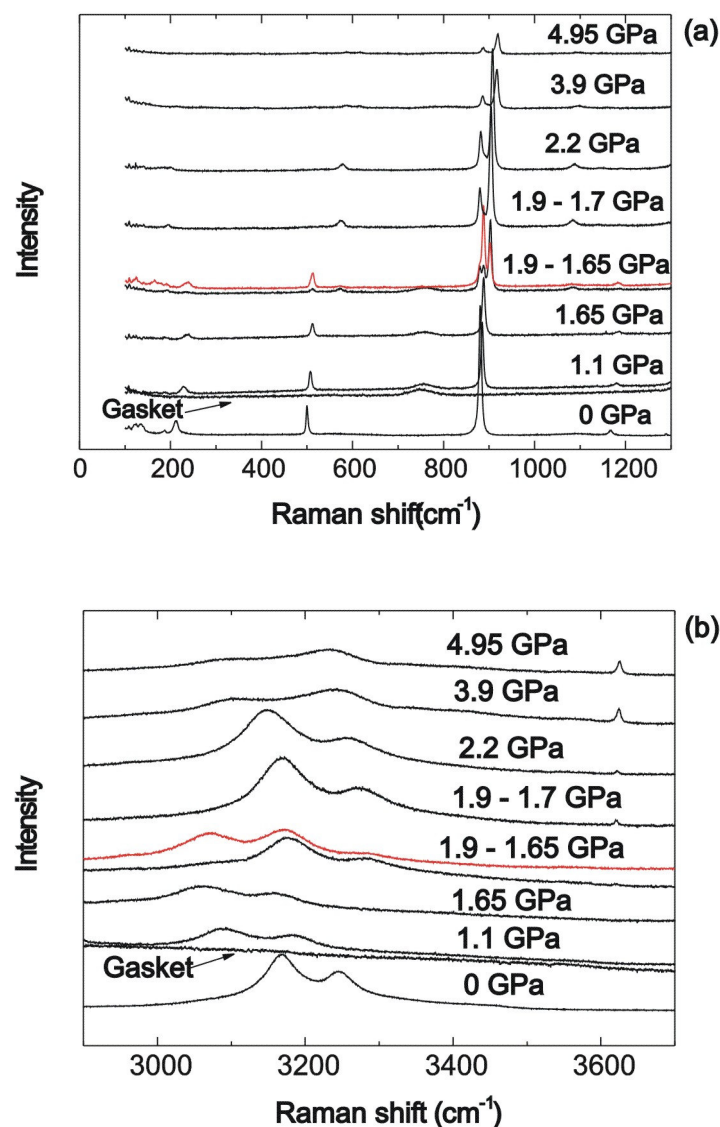

Figure 6: Pressure evolution of the Raman spectra for H_3BO_3 sample across the chemical decomposition on HBO_2 and H_2O (a) in the frequency range up to 1300 cm^{-1} and (b) from 2900 to 3700 cm^{-1} (higher magnification scale). The Raman spectrum of the gasket at 1.1 GPa is shown for comparison. The red and black spectra are taken in two different places of the sample at 1.65 GPa. The sample was initially compressed to 1.9 GPa and kept for 14 hours in a DAC.
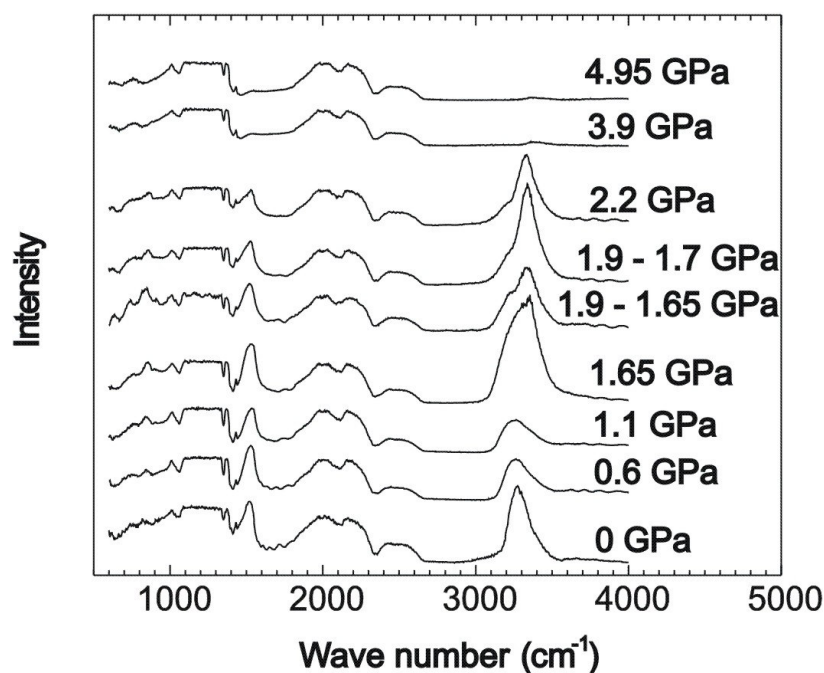
Figure 7. Pressure evolution of FTIR spectra for H_3BO_3 sample across the chemical decomposition on HBO_2 and H_2O.

IR spectra of the sample were dominated by the features coming from diamond and defects in a diamond structure in the ranges from 900 to 1400 cm^{-1} and from 1800 to 2700 cm^{-1} (Figure 7). Nevertheless, two infra-red active fundamental vibrations of boric acid could be identified in the regions of spectra free of diamond bands. The strong bands at 1520 and 3276 cm^{-1} in the ambient pressure IR spectrum can be assigned to the $v_{17}(E_{1u})$ B-O bond stretching mode and to the $v_{16}(E_{1u})$ O-H bond stretching vibration. The peak shape of these latter modes is clearly asymmetric which means a complex structure of the observed peak profiles.

Compression to about 1.6 GPa produces a continuous shift of the Raman and IR peaks described above in the respective spectra. In case of the Raman active $v_{23}(E_{2g})$, $v_3(A_g)$, $v_{22}(E_{2g})$ modes and the IR active $v_{17}(E_{1u})$ mode this shift is towards higher frequency (blue-shift), whereas the Raman and IR active bands related to the O-H bond stretching are shifted towards lower frequency. The chemical decomposition of H_3BO_3 was marked by appearance of new peaks in Raman and IR spectra at pressures above 1.6 GPa. The pressure of the sample varied during the decomposition process and was kept for about 15 hours within the 1.6–1.9 GPa range during successive data collections, analogously to the X-ray diffraction study. The new bands at 194, 576, 880, 905, 1085 cm^{-1} in the Figure 6(a) and at 3170, 3277, 3621 cm^{-1} in the Figure 6(b) progressively substitute the peaks originated from H_3BO_3 during its decomposition. The rise of the new peak at 3340 cm^{-1} could be observed also in the IR spectra during decomposition. Further pressure increase up to about 5 GPa resulted in a continuous frequency shift of the new bands in Raman and IR spectra. Due to a very limited information about the Raman and infrared spectra of γ-HBO_2 (Bertoluzza, 1980), the assignment of the observed Raman and IR bands which replace the peaks of H_3BO_3 can not be done unambiguously. A softening on compression of the Raman bands observed at 3170 and 3277 cm^{-1} at 1.9 GPa (fig. 6b) is a specific feature of a hydrogen bond in ice-VII (Walrafen, 1982). Consequently, these two peaks can be assigned to the $v_1(A_{1g})$ symmetric stretching and $v_3(E_g)$ antisymmetric stretching of the H_2O molecule (Pruzan, 1990). Additional study is required to precise the origin of the other Raman peaks observed in figure 6 during and after decomposition of H_3BO_3.

Conclusions

X-ray diffraction study showed that compressed to about 2 GPa boric acid, H_3BO_3, decomposes on cubic metaboric acid, HBO_2, and two structural modifications of ice, ice VI and ice VII. A polymorphic transformation of H_3BO_3 precedes the chemical decomposition which involves a big overall volume reduction. Complementary Raman and IR spectroscopy measurements are consistent with the results of X-ray diffraction study. The high-pressure Raman and IR spectra suggest that the $B(OH)_3$ molecular complexes of boric acid preserve their structure up to the pressure of the decomposition (around 1.6 GPa). The molecular H_3BO_3 crystal remains stable at pressures below than 1.6 GPa despite of the large volume variation which one can expect in this pressure range, as follows from the X-ray data (fig. 3). The reason of this stability can be attributed to kinetic requirements for the $H_3BO_3 \rightarrow HBO_2 + H_2O$ chemical reaction, which is not observed at low pressures and ambient temperatures. A big separation between the oxygen atoms situated in adjacent sheets of $B(OH)_3$ molecular complexes prevents a formation of hydrogen bonds in the direction of stacking of sheets. One can estimate from the data of figure 3 the pressure variation of the inter-layer O-O distances. The shortest inter-layer O-O distance becomes comparable with the intra-layer O-O distances at about 2 GPa. Consequently, the activation barrier for the hydrogen bond formation in this direction should be low enough to trigger a pressure induced decomposition of H_3BO_3 on more stable hydrogen bonded components, HBO_2 and H_2O.

References

Bertoluzza A., Monti P., Battaglia M. A., Bonora S. *J. Mol. Struct.* 64, 123 (1980).

Bethell D. E. *Trans. Faraday Soc.* 51, 9 (1955).

Birch F. *J. Geophys. Res.* 83, 1257 (1978).

Bromiley G. D., Keppler H., McCammon C., Bromiley F. A., Jacobsen S. D. *American Mineralogist* 89, 941 (2004)

Erdemir A., Bindal C., Zuiker C., Zavrun E. *Surf. Coat. Technol.* 86-87, 507 (1996).

Freyhardt C.C., Wiebcke M., Felsche J. *Acta Crystallogr.* C56, 276 (2000).

Hammersley A. P., Svensson S. O., Hanfland M., Fitch A. N., Hausermann D. *High Press. Res.* 14, 235 (1996).

Kracek F. C., Morey G. W., Merwin H. E. *Am. J. Sci.* A 235, 143 (1938).

McCalla E., Brüning R. *J. Mater. Res.* 17 (12), 3098 (2002).

Pereira A. S., Perottoni C. A., Da Jornada J. A. H. *J. Raman Spectrosc.* 34, 578 (2003).

Pereira A. S.. Haines J., Da Jornada J. A. H., Kuznetsov A. Yu., to be published.

Pruzan P., Chervin J.C., Gauthier M. *Europhys. Lett.* 13, 81 (1990).

Shuvalov R. R., Burns P.C. *Acta Crystallogr..* C59, i47 (2003).

Walrafen G.E., Abebe M. *J. Chem. Phys.* 77, 2166 (1982).

Zachariasen W. H. *Acta Crystallogr.* 7, 305 (1954).

Zachariasen W. H. *Acta Crystallogr.* 16, 380 (1963).

Zaki K., Pouchan C. *Chem. Phys. Lett.* 236, 184 (1995).

Zapol P., Curtiss L. A., Erdemir A.. *J. Chem. Phys.* 113, 3338 (2000).